The Development of a Low Mass Extendible Composite Boom for Small Satellite Applications

The Development of a Low Mass Extendible Composite Boom for Small Satellite Applications

Juan Reveles, Mike Lawton, Vincent Fraux, Vinoth Gurusamy

Oxford Space Systems Ltd.
Harwell Space Cluster, Harwell OX11 0QR, United Kingdom, +44(0)1235 567 999
juan.reveles@oxfordspacesystems.com

ABSTRACT

This paper describes an extendable boom structure which combines novel materials and proven actuation principles to deploy a low mass, high stowage efficiency motion structure. The extendable architecture presented incorporates a novel deployment mechanism for actuation and a novel flexible composite material for the boom element. The boom element itself possesses very low length-density and highly tuneable bending and torsional stiffness characteristics.

The total mass of the boom and mechanism arrangement is approximately 0.30Kg, the boom is retractable and can extend up to a 2m length from a stowage volume equivalent to less than half of 1U. The deployment can be achieved with less than 0.5W power consumption assuming vertical deployment with no gravity compensation and a 0.025kg payload.

Due to its low mass and high stowage efficiency the extendable boom design presented is well suited to small satellite applications where requirements for volume and mass are key design drivers. The architecture is versatile and thus can be used as an extendable boom for low mass and low positional accuracy payload requirements or can be used as an actuator as part of a larger, rigid multi-element telescopic boom for mission where stiffness and high positional accuracy are the main system drivers.

INTRODUCTION

Space missions often require a payload to be positioned away from the main body of a spacecraft; an obvious example being that of a magnetometer where the ability to distance the instrument from the disruptive electromagnetic field of the spacecraft reduces interference by the square of deployed distance achieved. Considering antenna applications where transmission and reception are handled by separate elements, it is advantageous to achieve a high level of spatial separation between elements in order to reduce crosslink by deploying the elements as far apart as possible. However, the challenges presented by the cubesat form factor means that deployable elements, although highly desired, are often compromised by the stowage volume available. This paper introduces an actuated linear flexible composite member that is compatible with the cubesat platform form factor and can be employed to realise a range of deployable structure requirements. In its simplest form, the flexible composite member can be used to position a payload in a controlled manner and with minimum shock to the platform. The deployable element is retractable, this feature decreases the risk of undesirable dynamic coupling with the platform by controlling the boom's length and thereby its torsional and bending stiffness and natural frequency characteristics. When additional structures are embedded within the boom material, such as cables or flexible printed circuit boards, more complex electrically active payloads can be realised without compromising the stowage volume of the flexible composite member. The extendable boom structure presented in this paper combines novel materials and proven actuation principles to deploy a low mass, high stowage efficiency motion structure. The boom element possesses very low length-density and highly tuneable bending and torsional stiffness characteristics. In this particular embodiment, the boom payload is supported by two additional sub-payloads; a magnetometer and RADFETs. The total mass of the boom and mechanism arrangement is approximately 0.30Kg, the current boom is retractable and can extend up to a 2m length from a stowage volume equivalent to less than half of 1U. Firstly a design description is provided, then some results focusing on the analytical characterization of the boom are presented and lastly an alternative boom architecture is introduced.

DESIGN DESCRIPTION

The boom payload comprises the following sub-systems:

- 2m long extendible rolled composite boom, boom mechanism, and associated controller PCB.
- Magnetometer and associated electronic circuit
- 2x RADFET (Radiation-Sensing Field-Effect Transistor) and associated electronic circuit

The extendible element of the boom sub-system is a 20mm diameter open-section flexible composite member with a 224° subtended angle and 0.3mm thickness. Epoxy-based plain weave carbon fibre prepreg has been used in the manufacturing of the boom as this material type has low outgassing characteristics and relatively high radiation tolerance, consistent with space environment requirements. The boom element itself can be fully deployed or only partially deployed; it can be retracted from any of these two states with controlled achieved via an optical encoder.

The magnetometer sub-payload is based on fluxgate magnetometer with driving analogue circuits and high precision/high speed 20 bit ADC.

The RADFETs (Radiation-Sensing Field-Effect Transistor) are microminitaure silicon pMOSFET transistors which act as an integrating dosimeter, measuring dose in rad or Gy(Si) by virtue of the field effect caused by space charge trapped in an inorganic insulator (SiO_2). The radiation-induced charge remains stored for many years.

The boom payload and sub-payloads fit within a standard 1U cubesat platform volume and its calculated maximum mass is approximately 0.75kg.

Mechanical Design

The mechanical components are manufactured using Alocromed aluminium alloy 6061T6 or the European equivalent 6082T6. Where low friction is required (e.g. components that interface with the composite boom), delrin-acetal is used instead. The payload consists of two 1.6mm thickness FR4 PCBs, the controller PCB drives the operation of the boom mechanism and the upper sub-payload PCB regulates the operation of the magnetometer and the RADFETs. The main structural components of the boom payload are the front plate and the mechanism retention plate (or back plate). A stiffener bracket connecting the front and back plates has been included to ensure the distance between these two components is preserved under transient mechanical loading. This bracket also increases the stiffness of the assembly considerably. Separation between the PCBs and between the controller PCB and the interface bracket is achieved via GRP stand-offs.

In the current mission, the boom is deployed along the Nadir pointing +Z axis, Figure 1 shows the payload and its axis definition.

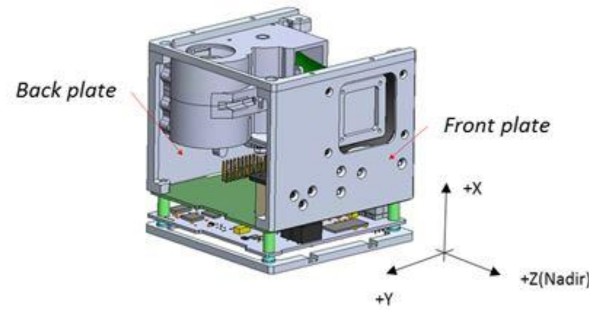

Figure 1: Boom payload geometry and axis definition

A detailed view of all other mechanical components is presented in Figure 2. These include a delrin bracket which has been designed to minimise the out-of-plane displacement of the PCB-mounted magnetometer under dynamic loading. An aluminium bracket has been included to mechanically support the drive motor with gearhead and encoder arrangement to avoid a cantilever configuration of a relatively heavy and sensitive component.

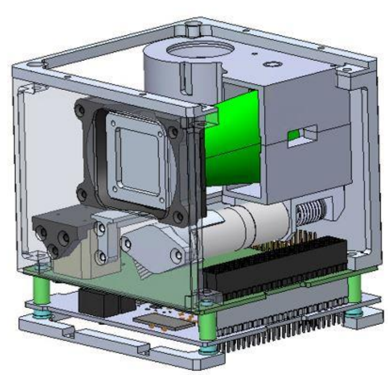

Figure 2: Mechanical components of the boom payload

From its stowed configuration the boom deploys through the retention cone: a conical-surfaced acetal component that houses the boom end plate during launch and during fully-stowed modes. Two boom trim plates are located in the retention cone as depicted in Figure 3. These trim plates allow adjustments to the orientation of the boom to ensure deployment occurs perpendicular to the XY plane. Inevitably some friction will be experienced between the boom and the trim plates and for this reason acetal has been selected for their construction.

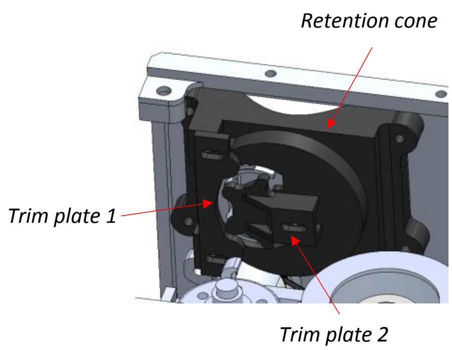

Figure 3: Boom retention feature and trim plates

Electronics Design

The boom payload PCBs consist of a primary system & secondary system with independent sensing circuits, data storage and power supplies. The I^2C spacecraft interface is the primary link with the OBC for both primary and sub-payloads.

• The primary system consists of an STM32F429 series microcontroller running at a maximum clock rate of 180 MHz, a 64 MB NAND flash, an 8 MB SD RAM, the primary motor control, three 20 bit ADCs running at a maximum rate of 1 MSPS, and switches to control the sub-payloads. The 5V rail from the spacecraft interface powers the motor control circuits and the 20 bit ADCs, while the rest of the systems are powered by 3.3V rail. The primary system is switched on by the spacecraft switch 1. The MCU has 12 bit ADCs, 16 channels programmed to run at 200 ksps which is used for internal current monitors, temperature monitors, calibrations and performance monitoring. The clock speed of the MCU can be changed according to the current task. The MCU and RAM combination will perform FFTs and different types of data compression, based on the type of data collected. A high precision optical encoder monitors the position of the boom. The encoder is self-calibrated with 2 end stops at the stowed and deployed position of the boom. The controller PCB can also connect to an external GPS if available.

• The sub-payload PCB consists of a STM32L151 series microcontroller running at a max clock of 32 MHz, 64 MB NAND flash, redundant boom motor control and power switches to control various sub payloads. The battery rail from the spacecraft interface powers all the systems through a switch mode regulator. The secondary system is switched on by the spacecraft switch 2. The MCU has 12 bit ADCs, 16 channels programed to run at 50 ksps which is used for internal current monitoring, temperature monitoring, calibrations and performance monitoring. The clock speed of the MCU will be changed according to the current task to minimise power drain on the spacecraft bus. The MCU can perform a limited data compression.

Mechanism Design

The mechanism itself is a positive drive system which guarantees deployment of the boom by engaging a multi-peg cog into the composite boom holes. The expected peak deploment torque is approximately 130Nmm and the expected peak retraction torque has been esimated at 200Nmm. With the current worm and transmission design this leads to a minimum required operational output torque of approximately 26Nmm for stowage and 17Nmm for deployment. With the current 9V drive system, a stall torque of approximately 60Nmm is expected. This provides a margin of 3.5 during deployment and 2.3 for stowage.

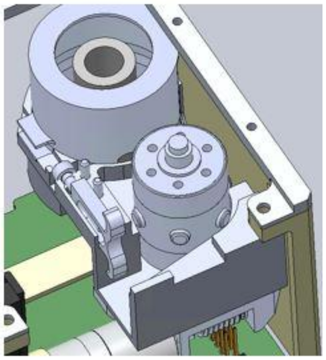

Figure 4: Cog of the drive mechanism

Accommodation

The boom and sub-payloads fit within a 1U volume and interfaces mechanically with the platform via two Al6061T6 brackets consistent with the current cubesat standard as depicted in Figure 5. Access to the mounting holes of the payload is available by virtue of the PCB standoffs and the separation between the controller PCB (lower) and the bottom mounting bracket. The integration of the payload to the platform is achieved via eight M3 screws that secure the unit to the platform structural frame. The payload itself is supplied as a standalone unit bounded by two Al6061T6 brackets. The main structural components (e.g. the back plate and the front plate) are attached to these brackets via another eight corner M3 screws which do not interface with the rest of the platform. The torque levels ensure there is no slipping or gapping between the unit and the mechanical interface during launch.

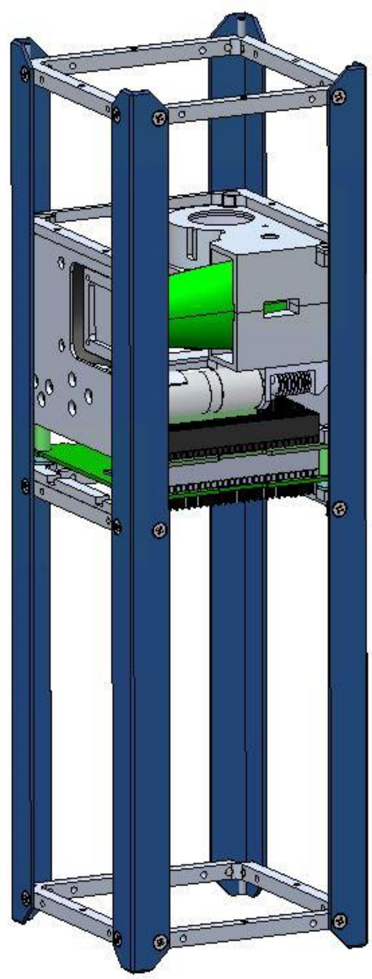

Figure 5: Accommodation of the payload in a cubesat structure

MECHANICAL ANALYSIS

Boom Stiffness Characteristics

The extendible element of the boom sub-system is a 20mm diameter open-section flexible composite member with a 224° subtended angle and 0.3mm thickness. The stiffness characteristics of the boom element are very tuneable. Structural torsional and bending stiffness, together with their associated natural frequencies, are depicted as a function of the subtended angle in Figure 6 through to Figure 9 for a 1m long boom and a multi-ply arrangement. The frequency results presented here correspond to a boom with the specified geometric characteristics and material layup without payload. There are approaches other than changing the boom geometry to tuning the stiffness, for example changing the number of plies, ply orientation, fibre type and resin matrix. However, these parameters are often limited by availability of raw materials, manufacturability and commercial constraints.

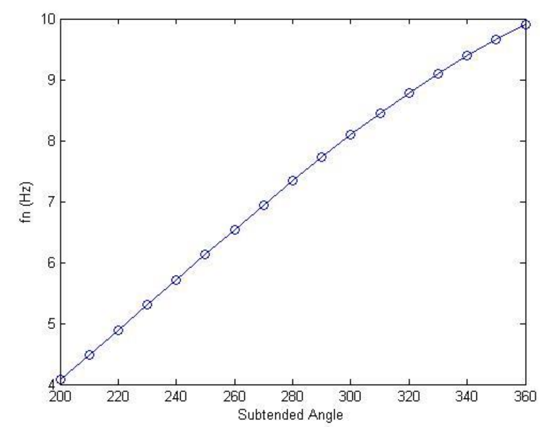

Figure 6: Bending frequency as a function of subtended angle

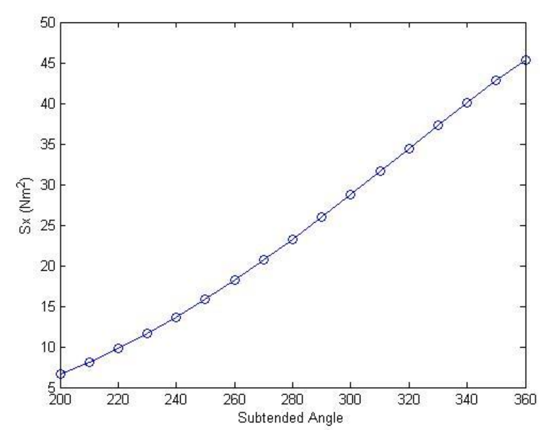

Figure 7: Structural bending stiffness as a function of subtended angle

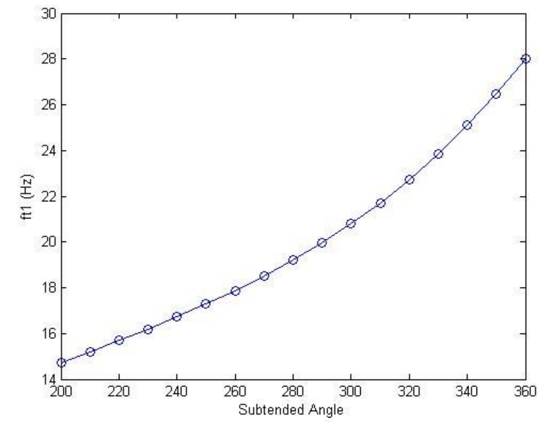

Figure 8: Torsional frequency as function of subtended angle

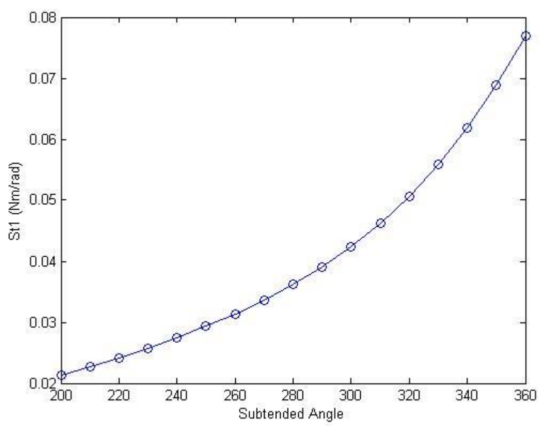

Figure 9: Structural torsional stiffness as a function of subtended angle

Payload Dynamic Characteristics

The payload structure has undergone modal finite element analysis in order to establish the dynamic characteristics of the system. All components that contribute to the overall stiffness of the payload unit have been included in the model. Components that do not contribute significantly to the stiffness and are regarded as non-structural mass have been included as point masses which attach to their support brackets. The boom motor, gearhead and encoder fall into this category. The PCBs have also been included and the non-structural mass has been distributed uniformly by increasing the overall density of the component. The finite element model of the payload consists of 170,199 solid tetrahedral elements, with 93.4% above an acceptable aspect ratio. The total number of nodes with is 291,449 and the number of DOF is 877,179.

Figure 10: FE model for analysis

The modal analysis was run for the first 45 modes. This resulted in a frequency range of 278Hz to 2,496Hz and a total accumulated mass participation of 94.6% along the X axis, 87.5% along the Y axis and 94% along the Z axis. The first mode corresponded to the controller PCB (lower PCB). This mode carried a mass participation of 12.6% and was an out-of-plane motion along the X axis, Figure 11.

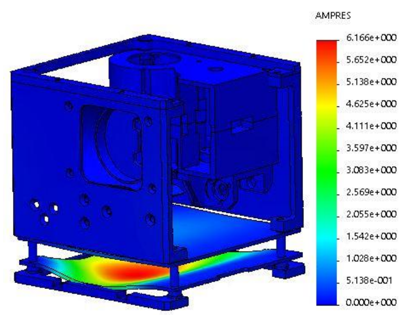

Figure 11: First mode (lower PCB)

The first structural mode occurred at 377Hz predominantly along the Z axis (52% of mass participation) although this mode was coupled as there was approximately a 12% mass participation along the X axis. This mode is depicted in Figure 12.

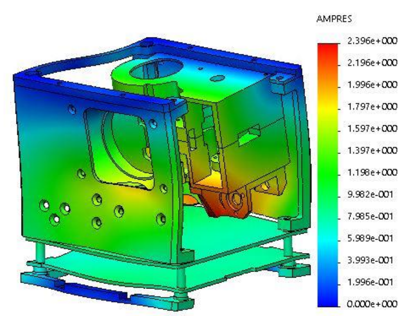

Figure 12: First structural mode (3rd overall)

Preliminary Assessment of Response to Random Excitation

The random base excitation in the GSFC Standard, Table 2.4-3 was used as input base excitation for a SDOF system with a fundamental frequency of 278Hz which simulated the controller PCB. The assumption was that this PCB exhibited SDOF behaviour and that there was no amplification or attenuation of the signal provided in Table 2.4-3. The dynamic response is presented in Figure 13 for a modal damping value of 3% which has been selected based on experimental values for PCBs where the typical amplification factor can be approximated as follows:

$$Q = \sqrt{f_n} \tag{1}$$

where Q is the amplification factor and f_n is the natural frequency of the PCB. In turn, the amplification factor is related to the modal damping as follows:

$$Q = \frac{1}{2\gamma} \tag{2}$$

with γ as the damping ratio.

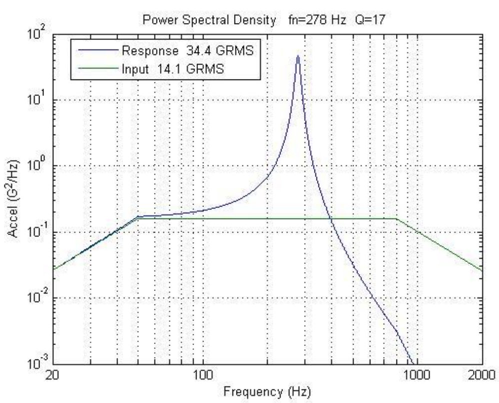

Figure 13: SDOF preliminary assessment of the PCB response to random vibration base excitation

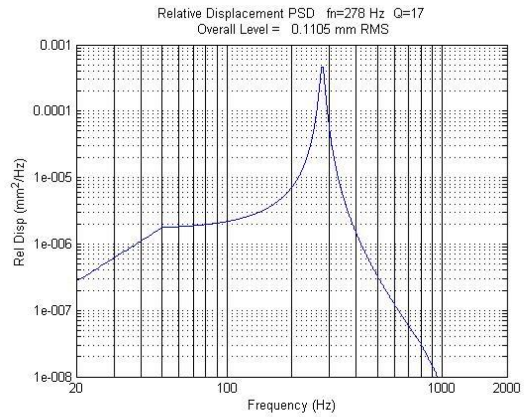

Figure 14: SDOF displacement response to random base excitation

An equivalent analysis was conducted for the first structural mode at 377Hz (treated as a SDOF system). The resulting gRMS was used on a 3 sigma equivalent body force static analysis. The dynamic response for an amplification factor of Q=10 is depicted in Figure 15.

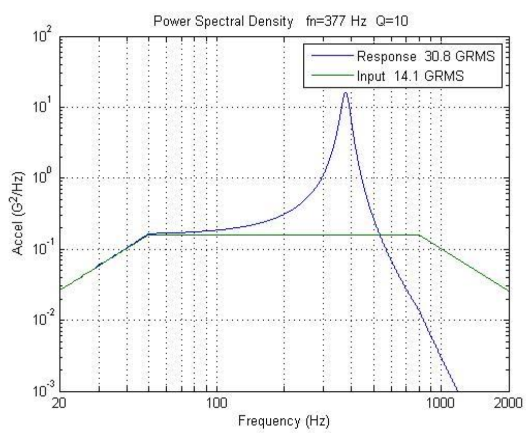

Figure 15: SDOF preliminary assessment of the structure's response to random base excitation

The resulting accelerations were used to verify the structural integrity of the payload under an equivalent body force in a 3 sigma analysis. The results indicated that the equivalent tensile stress of all components were within the material allowables. The FE model results are depicted in Figure 16 and Figure 17.

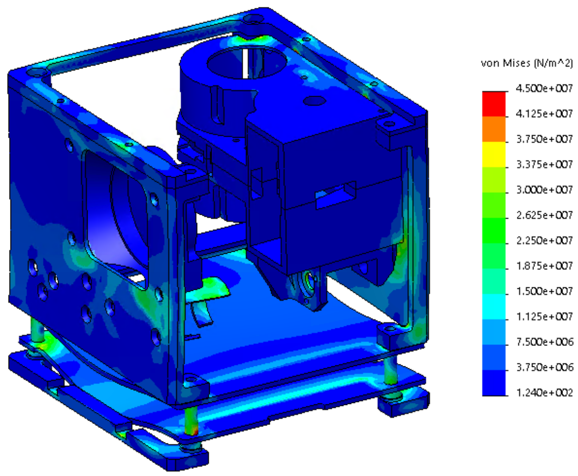

Figure 16: Resulting equivalent tensile stresses for a 3sigma output gRMS along the X axis

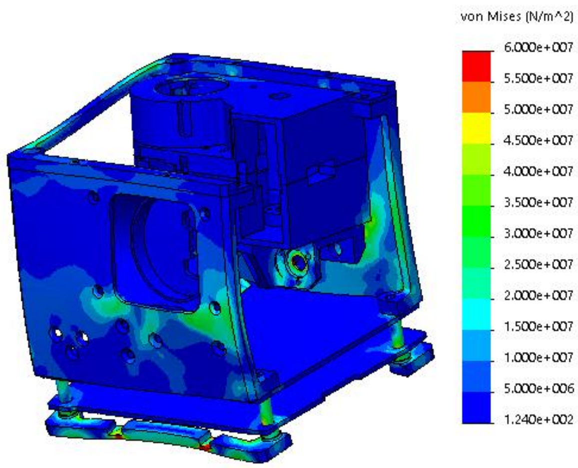

Figure 17: Resulting equivalent tensile stresses for a 3sigma output gRMS along the Z axis

OPERATIONAL MODES

The main operational modes of the boom payload and sub-payloads are now described.

Start up

This is the mode at initial power up. When the OBC turns on the payload the MCU-1 on the controller PCB and MCU-2 on the sub-payload PCB are powered up. The MCUs check for safe mode operations, initialize the I^{2}C bus, read and load up any flags & errors and then enter standby mode. This mode is explained in detail in the following steps:

1. Safe mode delay time: 2 seconds
2. Start-up I^{2}C master wait time 2 seconds – OBC can command a stepwise power on sequence from this step.
3. Start-up and initialize SPI and NAND flash. Reads flags and errors from the flash and set up sub-payloads and the power up procedure after entering standby mode.

The power-up procedure is the same for both controller and sub-payload PCBs. If either system experiences a reset because of error or malfunction, this is recorded in the flash at each step. The power-up mode is a unidirectional transition and the system enters this mode when the OBC switches on the payload and exits into the standby mode. Total transition time will vary between 0.1 to 7 seconds depending on the number of sub-payloads enabled and error counters. In case of non-recoverable errors in flash or SPI the system times out after 7 seconds and enters standby mode. The MCUs along with the enabled sub-payload are at full speed with peak current and max power.

Standby

Depending on the flags set by the start-up mode, the system will enter one of the power modes or wait for a command from the OBC. At power up the system enters standby mode automatically. Transition to other power modes is by either start up flags or I^{2}C commands. The system can enter standby mode from any of the power modes on command. The MCUs ensure all payloads are in standby with very low power. Transition between power modes is less than 100 milliseconds.

Normal Operation

This mode is bidirectional and the transition is controlled on command. The MCU clocks up and down depending on the task. Normal operational mode will be mainly used for processor-intense tasks. This is the recommended mode for data compression, data processing and FFTs and high speed magnetometer measurements. The transition to this mode from an operational mode will be less than 10 milliseconds.

Slow Operation

This mode is bidirectional and the transition is controlled on command. All the sub payloads run at slow speeds to conserve power. The MCUs max clock is limited to 50%. The transition to this mode from an operational mode is less than 10 milliseconds.

Low Power Operation

This mode is bidirectional and the transition is controlled on command. The MCUs max clock is limited to about 20%. This mode is recommended for conserving power. External ADC, RAM, Flash and Transceivers are disabled for this mode. The transition to this mode is less than 10 milliseconds.

Active Boom

This mode is bidirectional and the transition to the mode is controlled on command. During boom deployment and retraction the sub-payloads run in low speed mode. When auto power controls are enabled and a boom command is issued, the system automatically changes state to this mode. The transition to this mode is less than 10 milliseconds.

Power Down

The power down mode is a unidirectional transition and the system enters this mode when the OBC send an I^2C command to shut down. Total transition time will vary between 0.5 to 3 seconds depending on the number of sub-payloads enabled and collected data. The sub-payload MCU shuts down. In case of any error the system times out after 3 seconds and enters power down state ready to be turned off.

APPLICATIONS OF THE TECHNOLOGY

The following end applications have been identified for the flexible composite member:

a) Stand- alone low cost / low complexity boom

b) Actuator for telescopic boom (for high mass payloads such as electric propulsion placement)

c) General purpose linear actuator

d) Stored energy/self-deploying member

The first case has been described in the previous paragraphs and a physical prototype is depicted in Figure 18. This boom, which consists of a flexible composite extendible member and a compact motorized mechanism, is suitable for low mass payload which do not require particularly high pointing accuracy.

For case b) the flexible composite does not form a boom by itself, but is instead used as an actuator that drives an outer stack of nested telescopic tubes from a stowed position to a deployed state. An EQM of this boom type has been manufactured and successfully tested by OSS. Results from the qualification test campaign will be provided in a subsequent paper.

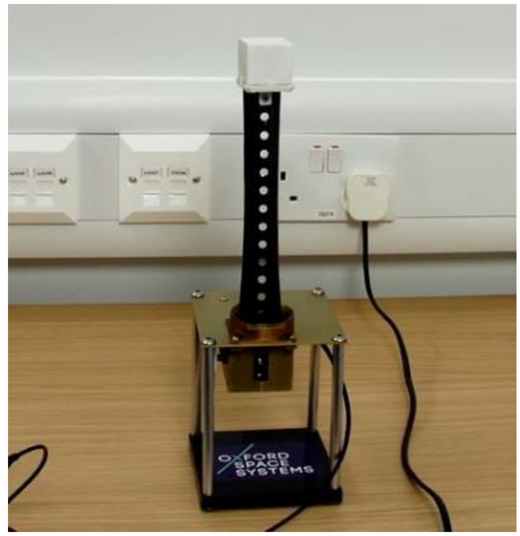

Figure 18: Low positional accuracy low mass boom

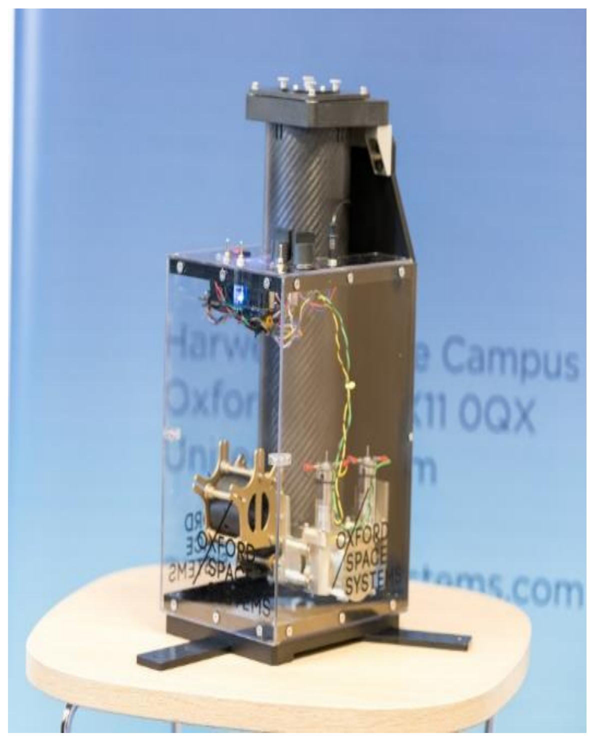

Figure 19: Boom in stowed position. The motorized flexible composite is used to drive a stack of nested tubes in a high precision, high stiffness and positional accuracy boom

Figure 20: 2.3m telescopic boom with flexible composite drive mechanism during deployment

References

1. Steinberg, D, Vibration Analysis for Electronic Equipment, John Wiley and Sons, Third Edition, Mexico, 2000.

2. ESA-ESTEC Requirements and Standards Division, European Cooperation for Space Standardization-Space Engineering-Structural Finite Element Models ECSS-E-ST-32-03C Netherlands, July 2008.

3. NASA GSFC, General Environmental Verification Standard for GSFC Flight Programs and Projects-GSFC-STD-7000, June 1996.